RNA Biology

ISSN: 1547-6286 (Print) 1555-8584 (Online) Journal homepage: http://www.tandfonline.com/loi/krnb20

Circular RNA Vav3 sponges gga-miR-375 to promote epithelial-mesenchymal transition

Xinheng Zhang, Yiming Yan, Wencheng Lin, Aijun Li, Huanmin Zhang, Xiaoya Lei, Zhenkai Dai, Xinjian Li, Hongxin Li, Weiguo Chen, Feng Chen, Jingyun Ma & Qingmei Xie

To cite this article: Xinheng Zhang, Yiming Yan, Wencheng Lin, Aijun Li, Huanmin Zhang, Xiaoya Lei, Zhenkai Dai, Xinjian Li, Hongxin Li, Weiguo Chen, Feng Chen, Jingyun Ma & Qingmei Xie (2019): Circular RNA Vav3 sponges gga-miR-375 to promote epithelial-mesenchymal transition, RNA Biology, DOI: 10.1080/15476286.2018.1564462

To link to this article: https://doi.org/10.1080/15476286.2018.1564462

Accepted author version posted online: 04 Jan 2019.

Publisher: Taylor & Francis

Journal: *RNA Biology*

DOI: 10.1080/15476286.2018.1564462

Circular RNA Vav3 sponges gga-miR-375 to promote epithelial-mesenchymal transition

Xinheng Zhang[1,4,5], Yiming Yan[1,4], Wencheng Lin[1,4,5], Aijun Li[2], Huanmin Zhang[3], Xiaoya Lei[1,4], Zhenkai Dai[1,4], Xinjian Li[1,4], Hongxin Li[1,4,5], Weiguo Chen[1,4,5], Feng Chen[1,4,5], Jingyun Ma[1,4,5], Qingmei Xie[1,4,5*]

[1]College of Animal Science, South China Agricultural University & Guangdong Provincial Key Lab of Agro-Animal Genomics and Molecular Breeding & Key Laboratory of Chicken Genetics, Breeding and Reproduction, Ministry of Agriculture, Guangzhou, 510642, P. R. China

[2]College of science and engineering, Jinan University, Guangzhou, 510632, P. R. China

[3]USDA, Agriculture Research Service, Avian Disease and Oncology Laboratory, East Lansing, MI, 48823, U.S.A.

[4]Key Laboratory of Animal Health Aquaculture and Environmental Control, Guangdong, Guangzhou, 510642, P. R. China

[5]South China Collaborative Innovation Center for Poultry Disease Control and Product Safety, Guangzhou, 510642, P. R. China

*Corresponding author: qmx@scau.edu.cn

Tel.: +86-20-8528-0283, Fax: +86-20-8528-0740

ABSTRACT

Circular RNAs (circRNAs) are evolutionarily conserved and widely present, but their functions remain largely unknown. Recent development has highlighted the importance of circRNAs as the sponge of microRNA (miRNA) in cancer. We previously reported that gga-miR-375 was downregulated in the liver tumors of chickens infected with avian leukosis virus subgroup J (ALV-J) by microRNA microarray assay. It can be reasonably assumed in accordance with previous studies that the gga-miR-375 may be related to circRNAs. However, the question as to which circRNA acts as the sponge for gga-miR-375 remains to be answered. In this study, circRNA sequencing results revealed that a circRNA Vav3 termed circ-Vav3 was upregulated in the liver tumors of chickens infected with ALV-J. In addition, RNA immunoprecipitation (RIP), biotinylated RNA pull-down and RNA-fluorescence *in situ* hybridization (RNA-FISH) experiments were conducted to confirm that circ-Vav3 serves as the sponge of gga-miR-375. Furthermore, we confirmed through dual luciferase reporter assay that YAP1 is the target gene of gga-miR-375. The effect of the sponge function of circ-Vav3 on its downstream genes has been further verified by our conclusion that the sponge function of circ-Vav3 can abrogate gga-miR-375 target gene YAP1 and increase the expression level of YAP1. We further confirmed that the circ-Vav3/gga-miR-375/YAP1 axis induces epithelial-mesenchymal transition (EMT) through influencing EMT markers to promote tumorigenesis. Finally, clinical ALV-J-induced tumor livers were collected to detect core gene

expression levels to provide a proof to the concluded tumorigenic mechanism. Together, our results suggest that circ-Vav3/gga-miR-375/YAP1 axis is another regulator of tumorigenesis.

Key words: Circ-Vav3, ALV-J, YAP1, gga-miR-375, EMT

Introduction

Circular RNAs (circRNAs) are a special class of endogenous RNAs which are covalently closed with their 3' and 5' ends joint together through exon or intron circularization [1, 2]. CircRNAs typically comprise exonic sequences and are spliced at canonical splice sites [3]. CircRNAs are more stable than linear RNAs and therefore may involve in different processes [4]. Recent studies have shown that circRNAs may relate to Alzheimer disease, prion disease and cancer [5-7], and there is accumulated evidence indicating that circRNAs can be associated with cancer-related miRNAs as a regulator of cancer-related pathways and can serve as diagnostic or predictive biomarkers of some cancers [8]. Although circRNAs are intensively studied, only a relatively small number of circRNAs have been assigned a function [9]. As such, it is extremely worthwhile to further explore the novel functional circRNAs in nature. MiRNAs are 21 to 23 nucleotide-long non-coding RNAs that guide the effector protein AGO2 to their target mRNAs to repress protein production [10-14]. MiRNAs are important regulators of gene expression at the post-transcriptional level and play important roles in tumorigenesis by regulating the expression of numerous genes associated with oncogenic signaling pathways [15]. MiR-375 is a well-established tumor suppressor microRNA that is downregulated in many types of cancer, and the downregulation of miR-375 has been proved to correlate with tumor size and invasion [16, 17]. The overexpression of miRNA-375 can inhibit tumor proliferation and induce apoptosis in papillary thyroid carcinoma cells [18].

Recently, circRNAs were identified to function as efficient microRNA (miRNA) sponges in an effector protein Argonaute 2 (AGO2)-dependent manner in mammals [19, 20]. Hence, miRNA-sponging is the only function discovered where the circular structure provides a unique advantage compared to linear RNA [9].

Yes-associated protein 1 (YAP1, an ortholog of Yorkie) is a key component of the Hippo signaling pathway in humans, which was initially identified as a mechanism that controls tissue growth and organ size in *Drosophila melanogaster*. It also functions as an oncogene in mammals [21, 22]. For instance, transgenic mice overexpressing YAP1 exhibit liver overgrowth and cancer development [23]. The ectopic expression of YAP1 promotes cell growth and oncogenic transformation *in vitro* [24]. It has also been proved by scientific research that YAP1 can regulate tumor survival and the epithelial-mesenchymal transition (EMT) [25]. The EMT is a highly conserved cellular program that is characterized by the phenotypic conversion of epithelial cells to mesenchymal cells and has more recently been proved to involve in cancer progression and metastasis [26]. A decline in the expression of E-cadherin in epithelial cells and the induction of Fibronectin, N-cadherin，Vimentin，ZEB1 and MMP2 in mesenchymal cells have been considered as the features of EMT [27, 28, 29, 30]. In addition, in recent years, numerous miRNAs have been shown to play integral roles in the modulation of the EMT [31], implying that looking for other molecules interacting with miRNA could also modulate the EMT.

Avian leukosis virus subgroup J (ALV-J), a prototypical member of the genus *Alpharetrovirus,* subfamily *Orthoretrovirinae,* family *Retroviridae*, causes diverse tumors such as myelocytomas, sarcomas, hemangiomas, nephromas and erythroblastosis, as well as

myeloid leukosis, leading to a high mortality rate among infected chickens [32-34]. The widespread distribution of divergent ALV-J strains has caused enormous economic losses, and the eradication of ALV-J remains a major challenge [35, 36]. ALV-J has been studied intensively, however, our understanding of the mechanisms of ALV-J-induced tumorigenesis is still limited [37].

In the present work, through circRNA sequencing, we identified a circRNA (circ-Vav3) whose expression was upregulated in ALV-J-induced tumor livers. Considering that our previous study confirmed the downregulation of gga-miR-375 in ALV-J-induced tumor livers [38], we are prompt to explore the relationship between circ-Vav3 and gga-miR-375 in tumorigenesis. For this purpose, we first verified circ-Vav3 as the sponge of gga-miR-375, after that, we continued to demonstrate how they promote tumor formation. Our data revealed that circ-Vav3 sponge function could elevate gga-miR-375 target gene YAP1. Further research confirmed that the circ-Vav3/gga-miR-375/YAP1 axis can affect EMT. In addition, we analyzed the expression of circ-Vav3, gga-miR-375, YAP1, E-cadherin, N-cadherin, Fibronectin, Vimentin, ZEB1 and MMP2 *in vitro* and *in vivo* after the host or host cells were infected with ALV-J. It is the first report that the circ-Vav3/gga-miR-375/YAP1 axis induces EMT to promote tumor formation.

Results

CircRNA expression profile and circRNA binding site prediction

Previously, our miRNA microarray results revealed gga-miR-375 was significantly downregulated in the liver of ALV-J-infected chickens compared to control chickens. The

miRNA expression profile was published as a heat map for nine selected miRNAs that were differentially expressed [38]. In this study, ALV-J-induced tumor livers from ALV-J-susceptible chickens and normal livers from ALV-J-resistance chickens at 10-weeks-old were used as circRNA sequencing samples (Fig. 1A) and circRNA sequencing revealed that a total of 13419 circRNAs were detected. Among those 13419 circRNAs, 2822 differentially expressed circRNAs (fold change ≥ 2，$P \leq 0.05$, FDR < 0.05) were detected in both tumor liver samples and normal liver samples by Volcano Plot, including 2808 differentially upregulated circRNAs that were identified in tumor liver samples (Figure 1B). Scatter plot analysis made the variation of circRNAs expressions of two groups be visualized in these plots (Figure 1C).

Based on relative levels in fold change (FC) and *P* value (FC ≥ 2.0 and *P* value ≤ 0.05), a total of 25 upregulated and differentially expressed circRNAs in ALV-J-induced tumor livers were selected to construct a heat map to illustrate the circRNA expression profiles (Fig. 1D). The 25 upregulated and differentially expressed circRNAs in ALV-J-induced tumor livers were listed in Table 1 and circ-Vav3 (chr8:1033880-1047222-) was significantly upregulated in ALV-J-induced tumor livers.

The predicted miRNA targets for the 25 differentially expressed circRNAs using TargetScan and miRanda [39, 40], only those miRNA response elements (MREs) predicted by both the algorithms were retained, and then ranked by pairing structure score derived from miRanda algorithm. The top five predicted miRNAs for every circRNA according to their pairing scores revealed that gga-miR-375 had the highest binding score to the circRNA circ-Vav3 (chr8:1033880-1047222-) (Table 2). Then, a circRNA-targeted miRNA-gene network using

three differentially expressed circRNAs was constructed to show the circRNA/miRNA relationships (Fig. 1E). In our previous study, RT-qPCR have confirmed the accuracy of the miRNA microarray and circRNA sequencing results including gga-miR-375 and circ-Vav3 [38, 41].

Circ-Vav3 sponges with miRNA-375

UCSC genome browser [42] was used for annotation of circ-Vav3 which is located between the eighth and eleventh exons of the annotated Vav3 gene region (Fig. 2A). Gga-miR-375 is predicted to have perfect target site complementarity with circ-Vav3 (Fig. 2B). RNA immunoprecipitation (RIP), biotin-coupled RNA pull-down and RNA-fluorescence *in situ* hybridization (RNA-FISH) assays were three methods to confirm the interaction between circRNAs and miRNAs [43-45] that we used to validate the interaction between circ-Vav3 and gga-miR-375. For RIP experiment, AGO2 and IgG beads were used to pull down AGO2 protein. AGO2 was successfully pulled down from the supernatants of the tumor liver samples, while AGO2 was not pulled down by the IgG beads in the negative control, this result illustrated that the negative control was properly set up. We further confirmed that the AGO2 protein could be successfully pulled down from the tumor liver samples (Fig. 2C and 2F). Next, we detected the presence of circ-Vav3 and gga-miR-375 in the AGO2 pull-down product. RT-qPCR showed circ-Vav3 was enriched by 59.81- and 56.87-fold, gga-miR-375 was enriched by 30.27-fold (U6 was the housekeeping gene) and 28-fold (5S was the housekeeping gene) respectively, in the AGO2 pull-down samples compared to the negative control (Fig. 2D, E, G, H), which suggests that circ-Vav3 binds to gga-miR-375 via AGO2

protein.

Moreover, biotin-labelled positive probe and negative probe of circ-Vav3 were synthesized and used to test whether the probes could pull-down gga-miR-375. RT-qPCR analysis of the probe pull-down samples showed that gga-miR-375 was enriched by 57.63 and 55.3-fold in the positive probe compared to that in the negative probe, U6 and 5S were used as the housekeeping gene (Fig. 2I, J*)*.

CircRNAs tend to accumulate in the cytoplasm of some cells and miRNAs are compartmentalized into the nucleus and cytoplasm, respectively [42, 46]. We performed RNA-FISH in DF-1 cells by co-incubation with biotin-labeled circ-Vav3 and digoxin-labeled gga-miR-375 probes to determine their subcellular localization. Circ-Vav3 distributed throughout the cytoplasm, while gga-miR-375 was detected in both the nucleus and cytoplasm. There was a large degree of overlap in the distribution of circ-Vav3 and gga-miR-375 (Fig. 2K), which suggests that circ-Vav3 and gga-miR-375 co-localize in the cytoplasm. These results indicate that circ-Vav3 interacts with gga-miR-375 in the cytoplasm.

Gga-miR-375 negatively regulates YAP1 by binding to its 3'UTR and gga-miR-375 overexpression alleviates EMT

Target prediction indicated YAP1 was a potential gga-miR-375 target gene based on miRanda and Targetscan (Fig. 3A). In animals, miRNAs bind to the 3' UTRs of their target mRNAs and interfere with translation [47]. The luciferase reporter gene assay has recently been adapted to test the effect of miRNAs on target mRNAs [48]. To confirm the predicted gga-miR-375-binding site in the 3'UTR of YAP1 mRNA, a luciferase reporter vector

containing the wild-type YAP1 3'UTR that is complementary to gga-miR-375 was constructed (Fig. 3A). A mutant reporter vector containing mutated YAP1 3'UTR that has no complementarity to gga-miR-375 was also constructed as a control. The reporter vector and gga-miR-375 precursor were co-transfected into DF-1 cells. A scramble control of gga-miR-375 (gga-miR-NC) was included as a control. Normal DF-1 cells were also set up as a control. Cells co-transfected with the gga-miR-375 precursor and wild-type YAP1 3'UTR exhibited significantly lower luciferase activity compared to gga-miR-NC or normal DF-1 cells ($P < 0.01$) (Fig. 3B). However, transfection of the mutant YAP1 3'UTR and gga-miR-375 had minimum effect on the luciferase activity compared to cells transfected with gga-miR-NC or normal DF-1 cells (Fig. 3B).

It has been reported that most animal miRNAs are imprecisely complementary to their mRNA targets and can inhibit protein synthesis [11], to text the effect of gga-miR-375 on its target YAP1, we transfected DF-1 cells with the gga-miR-375 mimic. Firstly, RT-qPCR was conducted to confirm that gga-miR-375 was successfully overexpressed compared to gga-miR-NC and mock-transfected cells (Fig. 3C). Furthermore, RT-qPCR showed overexpression of gga-miR-375 significantly decreased the mRNA level of YAP1 compared to gga-miR-NC and mock-transfected cells at 24h (Fig. 3D). Western blotting also showed overexpression of gga-miR-375 significantly suppressed the protein expression of YAP1 compared to gga-miR-NC at 48h (Fig. 3E). Our results are consistent with the idea that miRNAs function by sequestering protein production from targeted mRNAs [49]. Overall, these results indicate gga-miR-375 negatively regulates YAP1 protein expression by binding directly to the 3' UTR of YAP1 mRNA.

EMT is viewed as an essential early step in tumor metastasis [28] and induction of EMT commonly companied with up-regulation of N-cadherin, Fibronectin, MMP2, ZEB1 and Vimentin, while down-regulation of E-cadherin [30, 50, 51]. To assess whether gga-miR-375 influences the EMT, we transfected DF-1 cells with the gga-miR-375 mimic or gga-miR-NC. Western blotting showed overexpression of gga-miR-375 decreased the protein levels of N-cadherin, Fibronectin, Vimentin, ZEB1 and MMP2 to 42.67%, 31.67%, 40.67%, 43% and 23%, but increased the level of E-cadherin to 1.46-fold compared to the cells transfected with gga-miR-NC at 48h (Fig. 3F). RT-qPCR (Fig. 3G) showed that gga-miR-375 decreased the mRNA levels of Fibronectin, N-cadherin, ZEB1, MMP2 and Vimentin, to 41.38%, 28.89%, 23%, 38% and 28% but increased the level of E-cadherin to 2.22-fold compared to the cells transfected with gga-miR-NC and mock-transfected cells at 24h. These results demonstrate that instead of inducing EMT, gga-miR-375 alleviates EMT through down-regulation of N-cadherin, Fibronectin, Vimentin, ZEB1 and MMP2, while through up-regulation of E-cadherin.

MiRanda and Targetscan，two target prediction software were also used to research whether N-cadherin, Fibronectin, Vimentin, ZEB1 and MMP2 are the direct targets of gga-miR-375. The prediction results showed that they were not the target genes of gga-miR-375. The above results indicate that gga-miR-375 affects EMT possibly through a direct process where it upregulates gene YAP1 which then induces EMT.

YAP1 overexpression facilitates EMT and promotes cell migration in vitro

The collective migration of cells as a cohesive group is a hallmark of the tissue remodeling

events that underlie cancer invasion [52]. Next, we assessed the effects of YAP1 on the migration of DF-1 cells *in vitro*. Transwell assays showed overexpression of YAP1 increased the number of cells that migrated into the lower chamber compared to empty vector (EV) and mock-transfected cells (Fig. 4A, B). As the YAP1 was crucial for tumor maintenance, EMT plays a crucial role in tumor cell migration and elevation of YAP1 in epithelial cells also increased the number of tumor-promoting cancer-associated fibroblasts [53], we wanted to analyze whether overexpression of YAP1 could induce EMT in DF-cells. Western blotting (Fig. 4C) showed overexpression of YAP1 increased the levels of Vimentin, ZEB1, MMP2, Fibronectin and N-cadherin to 4.68-fold, 4.55-fold, 3.28-fold, 3.83-fold and 3.06-fold but decreased the level of E-cadherin to 25% compared to mock-transfected cells at 48h. RT-qPCR (Fig. 4D) showed overexpression of YAP1 increased the mRNA levels of Fibronectin, N-cadherin, Vimentin, ZEB1 and MMP2 to 1.69-fold, 3.28-fold, 2.79-fold, 2.85-fold and 3.39-fold but decreased the level of E-cadherin to 21.26% compared to mock-transfected cells at 24h. Taken together, these data suggest a functional role for YAP1 in facilitating EMT and cell migration in DF-1 cells.

Co-transfection with circ-Vav3 and gga-miR-375 facilitate EMT through enhancing YAP1 expression in DF-1 cells

CircRNAs bind to miRNAs and prevent these miRNAs from acting on their cognate targets have been reported previously [43, 54], to study the effect of circ-Vav3 sponges with gga-miR-375 on YAP1, we co-transfected circ-Vav3 and gga-miR-375 and the expression levels of EMT markers which could be affected by YAP1 [53] were first tested and then tested

the cognate target gene YAP1 expression level. We transfected DF-1 cells to overexpress gga-miR-375 in two groups, and then one group was transfected with PLCDH-circ-Vav3 as the treatment group and the other group was transfected with PLCDH-circ-EV (empty vector) as a control group. Firstly, the PLCDH-circ-Vav3 expression plasmid was successfully overexpressed in DF-1 cells to 9566-fold compared to the PLCDH-circ-EV group and mock group (Fig. 5A). Western blotting showed co-transfection of circ-Vav3 and gga-miR-375 significantly upregulated Fibronectin, N-cadherin, MMP2, ZEB1 and Vimentin by 2.24, 2.31, 2.60, 3.68 and 2.12-fold, respectively, and downregulated E-cadherin by 35% at 48h (Fig. 5B), these results were consistent with the requirement of facilitating EMT [47]. RT-qPCR showed co-transfection of circ-Vav3 and gga-miR-375 significantly increased Fibronectin, N-cadherin, ZEB1, MMP2 and Vimentin mRNA levels to 3.21, 3.98, 3.87, 2.88 and 3.09-fold, respectively, whereas significantly decreased E-cadherin mRNA level to 25.59% at 24h (Fig. 5C, D). Western blotting and RT-qPCR also showed co-transfection of circ-Vav3 and gga-miR-375 significantly increased YAP1 protein expression to 3.02-fold at 48h, and significantly increased YAP1 mRNA expression to 2.57-fold compared to cells transfected with the PLCDH-circ-EV and gga-miR-375 at 24h (Fig. 5B, D). As we have proved before that YAP1 up-regulation could facilitate EMT, the data of this part confirm and indicate that circ-Vav3 function as the gga-miR-375 sponge to induce EMT through positively upregulated gga-miR-375 target gene YAP1.

ALV-J upregulates circ-Vav3 and YAP1, downregulates gga-miR-375, facilitates EMT in vitro and affects their expression levels in clinical liver samples

Next, we assessed the effect of ALV-J on circ-Vav3, gga-miR-375, YAP1 and EMT-associated protein markers *in vitro*. Infection of DF-1 cells with ALV-J increased the level of circ-Vav3 at 12h to 3.1-fold compared to the mock-infected cells (Fig. 6A), but decreased the level of gga-miR-375 at 12 h to 42% compared to the mock-infected cells, while increased the level of gga-miR-375 in the mock-infected cells from 0 h to 12 h by 1.78-fold (Fig. 6B). Western blotting showed YAP1, Vimentin, ZEB1, MMP2, Fibronectin and N-cadherin were upregulated in ALV-J infected cells by 2.27, 1.99, 2.14, 2.51, 5.24 and 2.31-fold, respectively, whereas the epithelial marker E-cadherin was downregulated in ALV-J-infected cells to 43% compared to mock-infected cells at 48h (Fig. 6C). RT-qPCR showed that infection of DF-1 cells with ALV-J increased YAP1 mRNA levels to 1.86-fold at 24h (Fig. 6D), also increased Fibronectin, N-cadherin, Vimentin, MMP2 and ZEB1 mRNA levels to 1.53, 2.20, 2.48, 2.29 and 2.31-fold, respectively, whereas decreased E-cadherin mRNA level to 30% at 24h (Fig. 6E*)*. These data confirm ALV-J decreases the expression levels of gga-miR-375 and E-cadherin, while increases the expression levels of YAP1, N-cadherin, Fibronectin, Vimentin, ZEB1 and MMP2 *in vitro*.

Clinical samples were commonly used to confirm circRNAs expression level trends compared with that *in vitro* for validation clinical significances of those genes [55]. We next detected the expression levels of circ-Vav3, gga-miR-375, YAP1 and EMT markers by RT-qPCR using clinical liver samples including ALV-J-induced tumor livers and normal livers. We found that circ-Vav3 was upregulated in tumor livers by 19-fold compared to the normal livers ($P < 0.01$; Fig. 6F); gga-miR-375 was downregulated in tumor livers by 12-fold compared to the normal livers ($P < 0.01$; Fig. 6G); YAP1 was upregulated in tumor livers by

7.3-fold compared to the normal livers ($P < 0.01$; Fig. 6H); For EMT markers Fibronectin, N-cadherin, Vimentin, ZEB1 and MMP2, they were upregulated in tumor livers by 4.99, 4.01, 3.62, 4.28 and 4.55-fold, respectively compared to the normal livers ($P < 0.01$; Fig. 6I, J, L, M, N), however, E-cadherin marker level decreased 4.77-fold in tumor livers compared to the normal livers ($P < 0.01$; Fig. 6K).

Discussion

CircRNAs has been recently identified to have connections with numerous mammalian diseases [56, 57], and many researchers have shown great interest in exploring their functions. Some studies have revealed that a circRNA Foxo3 can promote cardiac senescence by modulating multiple factors associated with stress and senescence responses [58], while another research has confirmed that it has other functions in promoting breast cancer progression [59]. Cancer, as the most lethal disease, involves in abnormal cell growth to invade or spread to other parts of the body. Since the chance of being cured of cancer is very low, many scientists are dedicated to tackling this disease. Exploring biomarkers of cancers has always been a prioritized research area. In this study, we identified a circular RNA termed circ-Vav3 by circRNA sequencing from the myeloid tumor livers induced by ALV-J which is a retrovirus. To our knowledge, this is the first report of the existence of circ-Vav3 in nature and it triggers our interest in exploring the relationship between circ-Vav3 and tumor formation.

A number of mammalian circRNAs have been identified to function as effective miRNA sponges that relieve the inhibition of miRNA target gene expression [5, 60]. For instance, a study showed that circHIPK3 regulates cell growth by sponging multiple miRNAs [43].

Another research suggested that Hsa_circ_0005986 inhibits carcinogenesis by acting as a sponge of miR-129-5p and is used as a novel biomarker for hepatocellular carcinoma [61]. Based on our previously discovery which is that gga-miR-375 was differentially down-regulated in tumor livers, it is plausible that there is a sponge relationship between circ-Vav3 and gga-miR-375. Hence, in this study, we predicted the miR-375 binding sites of the differentially expressed circ-Vav3 using TargetScan and miRanda. To our surprise, there were total six seed sequences of circ-Vav3 that completely match with the gga-miR-375. We then further explored the sponge function of circ-Vav3 on gga-miR-375 with RIP, biotin-coupled RNA pull-down and RNA-FISH conducted as previously reported [43-45]. Here, it is worth mentioning that, apart from the confirmation the sponge function of circ-Vav3 on gga-miR-375 in an AGO2-dependent manner, we have also found that circ-Vav3 plays a sponge role in the cytoplasm. In our previous study, we demonstrated that circRNAs are play an important role in resisting ALV-J-induced tumor formation [41], while the purpose of this study, we aim to reveal that circRNAs are also participated in ALV-J-induced tumor formation according to analyzing circRNA expression profile and verifying tumorigenic function by a series of experiments. Although circular RNA sequencing result of circ-Vav3 has been confirmed by RT-qPCR in our previous report [41], however, its function has never been reported.

Since we have found that circ-Vav3 sponges with gga-miR-375, the further exploration of its effects on their downstream genes is the key to reveal the mechanism of tumorigenesis. In 2010, Liu reported that YAP1 was a direct target gene of miR-375, which was confirmed by luciferase reporter assay, and through immunoblotting, it was found that miR-375 can

suppress the level of endogenous YAP protein [62]. Consistently, it has been shown in this study that gga-miR-375 targets YAP1, and that the gga-miR-375 down-regulation can increase the level of endogenous YAP1 which has been identified as an oncogene contributing to cancer cell proliferation and which has also been proved to involve in the EMT [63, 64]. Our results indicate that gga-miR-375 down-regulation can promote tumor properties, which explains why gga-miR-375 level was decreased *in vitro* and *in vivo* after ALV-J infection. Since the gain of mesenchymal cell markers (Fibronectin, N-cadherin, Vimentin, ZEB1 and MMP2) and the loss of epithelial marker (E-cadherin) are regarded as the representative EMT markers [50], we examined the mRNA and protein expression levels of N-cadherin, Fibronectin, Vimentin, ZEB1, MMP2 and E-cadherin *in vitro* and *in vivo* to detect the EMT induction. It is noteworthy that we have proved that ALV-J is able to induce EMT not only through directly diminishing gga-miR-375 but also through the circ-Vav3 sponge function with gga-miR-375. Previous studies have confirmed that circRNA sponging with miRNA can relieve the inhibition of miRNA target gene expression [5, 60], then we assumed that it is the increase in the expression of the gga-miR-375 target gene-YAP1 that contributes to the EMT induction.

Furthermore, as understanding how YAP1 induces EMT in this study is of great importance, we detected Fibronectin, N-cadherin, Vimentin, ZEB1, MMP2 and E-cadherin expression level *in vitro*. As we expected, the overexpression of YAP1 can affect the three EMT markers at the same time. Most importantly, clinical ALV-J-induced tumor livers and normal livers were collected and core genes including circ-Vav3, gga-miR-375, YAP1, Fibronectin, N-cadherin, Vimentin, ZEB1, MMP2 and E-cadherin were detected. The expression levels of

these core genes in the livers were consistent with those *in vitro*. As such, we can present both *in vivo* and *in vitro* evidence that these core genes affect the development of tumorigenesis according to their expression trends.

In this study, we conclude that when circ-Vav3 is up-regulated in host cells which are infected with ALV-J, circ-Vav3 begins to act as the sponge of gga-mir-375 and relieve the inhibition of the gga-miR-375 target gene-YAP1which then induces EMT through affecting the mesenchymal and epithelial cell markers, and finally promotes tumorigenesis. To sum up, the circ-Vav3/gga-miR-375/YAP1 axis is a positive regulator to promote tumorigenesis through inducing EMT (Fig. 7). Revealing the pathogenic role of circ-Vav3 may offer a new potential therapeutic target to treat tumors. However, the expression level of circ-Vav3 and its sponge function in other types of cancers in nature needs to be further explored.

Materials and Methods

Ethics statement

The chicken study was carried out in accordance with the recommendations of the Guide for the Care and Use of Laboratory Animals of the National Institutes of Health. The use of the animals in this study was approved by South China Agricultural University Committee of Animal Experiments (approval ID: 201004152).

Samples, virus and cell lines

ALV-J-susceptible and -resistant chickens (F3 generation) were used as classical models of ALV-J-infected chickens (easily-induced tumors) or ALV-J-negative chickens

(tumor-resistance) in response to ALV-J challenge and the liver tissues of ALV-J-susceptible and –resistant chickens at 10 weeks were subjected to circular RNA sequencing [65]. Clinical samples including ALV-J-induced tumor livers (n=8) and normal livers (n=8) at 13 weeks were collected from chicken farms in Guangdong province for further genes expression levels test *in vitro*. The standard ALV-J NX0101 strain, which induces myeloid tumors, was used to infect chickens at one-day-old or DF-1 cells. Cells were cultured in Dulbecco's modified eagle medium (DMEM) supplemented with 10% fetal bovine serum (FBS; Invitrogen, Carlsbad, CA, USA).

CircRNA sequencing and target site prediction

CircRNA sequencing was performed as described previously [41]. Total RNA samples isolated from the liver of three chickens in each group and were treated with DNase I (Ambion Turbo DNA-free kit) and NucAway spin columns (Thermo Fisher Scientific) to remove DNA contamination and salts. The RNA was incubated at 70℃ for 5 min and then 3 μl of Rnase R was added and incubated at 37℃ for 10 min. After the reaction, the treated RNA was purified using the RNeasy MinElute Cleanup kits (Qiagen, Valencia, CA, USA) and Agencourt RNAClean XP (Beckman Coulter, Brea, CA, USA). RNA libraries were constructed from the treated RNAs using the TruSeq Stranded Total RNA Library Prep Kit (Illumina, San Diego, CA, USA) according to the manufacturer's instructions. Libraries were controlled for quality and quantified using a BioAnalyzer 2100 system (Agilent Technologies, Inc., Santa Clara, CA, USA). The libraries were denatured as single-stranded DNA molecules, captured on Illumina flow cells, amplified *in situ* as clusters and subjected to 150 sequencing cycles on an Illumina

HiSeq Sequencer. Microarray analysis of our previous study were used [38], the potential miRNA response elements (MREs) for the 25 differentially expressed circRNAs were identified using customized Arraystar miRNA target prediction software based on the miRanda and TargetScan algorithms [39, 40].

Reverse transcription and quantitative PCR (RT-qPCR)

Total RNA was extracted for circRNA analysis using RNAprep Pure Tissue Kit (TianGen Biotech Co., Ltd., Beijing, China) according to the manufacturer's instructions. MiRNAs were extracted using the mirVana miRNA Isolation Kit (Life Technologies, Carlsbad, CA, USA) following the manufacturer's instructions. Relative expression of circ-Vav3 and gga-miR-375 from the circular RNA sequencing and MiRNA microarray results have already confirmed using RT-qPCR [38, 41]. Relative expression of circ-Vav3, gga-miR-375, YAP1 and three EMT markers (N-cadherin，E-cadherin, Fibronectin) in DF-1 cells after ALV-J challenge or after transfection with gga-miR-375 mimic or co-transfection with circ-Vav3 and gga-miR-375 were also evaluated using RT-qPCR. β-actin and 5S were the housekeeping genes for circ-Vav3 and gga-miR-375 respectively. GAPDH was the housekeeping gene for YAP1 and three EMT markers. Circ-Vav3, gga-miR-375, YAP1 and EMT markers relative expression in clinical ALV-J-induced tumor livers and normal livers were also detected by RT-qPCR. Above mentioned primers used for RT-qPCR were listed in Table 3. The RT-qPCR data was analyzed as relative gene expression using the $2^{-\Delta\Delta Ct}$ method [66].

RNA immunoprecipitation, biotin-coupled RNA pull-down and RNA-FISH assay

Liver tissues from ALV-J-susceptible chickens were subjected to RNA immunoprecipitation (RIP), biotin-coupled RNA pull-down assays. An antibody against AGO2 (ab57113; Abcam, Cambridge, UK) was used for RIP using the Magna RIP™ RNA Binding Protein Immunoprecipitation kit (Millipore, Billerica, MA, USA). RNA was isolated using TRIzol reagent (Life Technologies) after formation of magnetic bead-antibody-gene complexes. Circ-Vav3, gga-miR-375, GAPDH (as the housekeeping gene for circ-Vav3), U6 and 5S (as the housekeeping genes for gga-miR-375) transcription were evaluated by RT-qPCR and the primers were listed in Table 4.

For biotin-coupled RNA pull-down assay, StreptavidinDyna beads (Dyna beads M-280 Streptavidin, #11205D, Thermo Fisher Scientific, Waltham, MA, USA) coated with biotin-labelled circ-Vav3 and negative probe were incubated with cell lysisand processed according to manufacturer's instructions. The sequence of positive probe and negative probe of circ-Vav3 were 5'-AAAGCATAATCTGGCCGTATATTTGACCTGGGTCCACGTGTCTGGAGTTCC-3' and 5'-AAAGGAACTCCAGACACGTGGACCCAGGTCAAATATACGGCCAGATTATGC-3', respectively. RNAs were eluted and reverse transcribed to cDNA. Gga-miR-375 expression was quantified by RT-qPCR. U6 and 5S were as the housekeeping genes for gga-miR-375.

A double RNA-FISH assay was performed in DF-1 cells. Biotin-labelled probes specific to circ-Vav3 and digoxin-labelled probes specific to gga-miR-375 (Exiqon, Vedbaek, Denmark) were used for hybridization. The probe sequences for circ-Vav3 and gga-miR-375 were 5'-CCGTATATTTGACCTGGGTCCACGT-3' and 5'-TAACGCGAGCCGAACGAACAAA-3', respectively. Probes were pre-denaturated at

88°C for 5 min followed by 3 min at 4°C. DF-1 cells were plated into 12-well plates containing cover glass and were cultured to the exponential phase (90% confluence), fixed, hybridized with probes for circ-Vav3 and gga-miR-375 at 37°C overnight, then incubated with anti-biotin-Rhodamine and anti-digoxin-FITC secondary antibodies for circ-Vav3 and gga-miR-375, respectively. Nuclei were counterstained with 4,6-diamidino-2-phenylindole (DAPI). Images were acquired using a Leica SP5 confocal microscope (Leica Micosystems, Mannheim, Germany).

Luciferase reporter vector construction

A fragment of the 3' UTR of wild-type YAP1 was amplified by RT-PCR using the primers 5'-TTCTCGAGGGAGATGGGATGAATATAGAAGG-3' and 5'-GGTGTCTAGACCACAGGCAGCAGGAGAC-3'. The region containing the putative binding sites for gga-miR-375 was inserted downstream of the stop codon of firefly luciferase in the pmiRGLO Dual-Luciferase miRNA Target Expression Vector (Promega, Madison, WI, USA) as described previously [67] (and designated YAP1-3'UTR-wt). PmiRGLO-YAP1-3'UTR-mut, which carries a mutated version of the complementary site for the seed region of gga-miR-375, was generated using the primers 5'-TTATCCCTCCTTTAAGTGAGATTCTCACAATTG-3' and 5'-TTAAAGGAGGGATAAAGGAGTTATGGGT-3' (and designated YAP1-3'UTR-mut).

Dual luciferase reporter assay

A Renilla luciferase expression construct and the pmiRGLO firefly luciferase expression

construct containing the 3' UTR sequence of YAP1 were used in the Dual luciferase reporter assay. DF-1 cells were cultured in 24-well plates, cotransfected with 10 nmol/L gga-miR-375 or miR-NC, 20 ng YAP1-3'UTR-wt or YAP1-3'UTR-mut, and 4 ng pRL-TK (Promega) using Lipofectamine 2000 (Thermo Fisher Scientific, Waltham, MA, USA) following the manufacturer's protocol. Cells were collected 48 h after transfection and analyzed using the Dual-Luciferase Reporter Assay System (Promega, Madison, WI, USA). Luciferase activity was detected using a Lumat LB 9507 Ultra Sensitive Tube Luminometer (Titertek Berthold, Nanjing, P. R. China) and the firefly luciferase activity of each sample was normalized to Renilla luciferase activity. Transfections were performed in duplicate and the experiments were repeated independently at least three times.

Plasmid constructs, RNA oligoribonucleotides and cell transfection

The empty PLCDH-ciR vector was used to construct the circ-Vav3 expression plasmid using the EcoRI and BamHI restriction enzyme sites. Primers for circ-Vav3 were 5'-cgGAATTCTGAAATATGCTATCTTACAGGTCAAATATACGGCCAGATTATG-3' and 5'-cgGGATCCTCAAGAAAAAATATATTCACCTGGGTCCACGTGTCTGGAGTTC-3'.

The PLCDH-circ-Vav3 expression plasmid was confirmed by sequencing.

To create pRK5-flag-YAP1, YAP1 mRNA was amplified by PCR using the primers 5'-TCTAGAATGGATCCAGG-3' and 5'-AAGCTTTCACAGCCATG-3', cloned into the pRK5-flag vector using Xbal and HindIII, and the vector was confirmed by sequencing. The gga-miR-375 mimic (UUUGUUCGUUCGGCUCGCGUUA) and mimic control duplexes (UUCUCCGAACGUGUCACGUTT) were designed and synthesized by GenePharma

(Shanghai, P. R. China). Co-transfection of PLCDH-circ-Vav3, pRK5-flag-YAP1 and RNA oligoribonucleotide(s) was performed using Lipofectamine 2000 reagent (Thermo Fisher Scientific, Waltham, MA, USA) following the manufacturer's protocol.

Western blotting analysis

DF-1 cells were subjected to western blotting analysis after transfection with gga-miR-375 and pRK5-flag-YAP1 using a polyclonal rabbit anti-YAP1 primary antibody (1:1000; Proteintech Group, Rosemont, IL, USA), monoclonal rabbit anti-N-cadherin antibody (1:1000; Abcam, Cambridge, UK), polyclonal goat anti-E-cadherin antibody (1:400; Santa Cruz Biotechnology Inc., Dallas, TX, USA), monoclonal mouse anti-Fibronectin antibody (1:1000; Millipore, Billerica, MA, USA). A β-actin antibody (1:1000; Bioss Antibodies, Woburn, MA, USA) was used as a loading control. The secondary antibodies were goat polyclonal anti-rabbit IgG (H+L)-horseradish peroxidase (HRP; Bioss Inc), polyclonal donkey anti-goat IgG-HRP (Santa Cruz Biotechnology Inc., Dallas, TX, USA), and rabbit polyclonal anti-mouse IgG-HRP (Biosharp, Heifei, China). Western blot bands were quantified with Image-Pro Plus 6.0 (Media Cybernetics Inc., Bethesda, MD, USA).

Cell migration

Cell migration assays were performed using Transwell chambers (Millipore, Billerica, MA, USA). Cells were harvested at 48 h post-transfection, and 5×10^4 cells were seeded in the upper chamber in 200 μL serum-free medium. The lower chamber was filled with medium supplemented with 10% FBS. Cells remaining on the upper membrane were removed after 12 h, and migratory cells on the bottom surface were fixed in 90% alcohol and stained with 0.1%

crystal violet. The numbers of cells in five random fields in each membrane were counted. Experiments were performed independently in triplicate.

Statistical analysis

Data were processed using GraphPad Prism (version 5.0; GraphPad software Inc, San Diego, CA, USA) and are expressed as the mean±s.e.m. The Student's *t*-test was used to assess differences between groups; $P < 0.01$ and $P \leq 0.05$ were considered significant.

Accession number

The circRNA data from this study was submitted to the National Center for Biotechnology Information's Gene Expression Omnibus (GEO) and was assigned the accession number GSE99286.

Disclosure statement

The authors declare that they have no conflict of interest.

Acknowledgments

We would like to thank Dr. Huanmin Zhang from USDA, Agriculture Research Service, Avian Disease and Oncology Laboratory for providing technical assistance in this study.

Funding

This study was supported by the National Natural Science Foundation of China (Grant Nos.

31672564, 31472217), International Science and technology cooperation project of Guangdong Province (2016A050502042), Construction project of modern agricultural science and technology innovation alliance in Guangdong Province (2018LM1112), and the Natural Science Foundation of Guangdong Province (Grant No. S2013030013313).

References

[1] Legnini I, Di Timoteo G, Rossi F, et al. Circ-ZNF609 is a circular RNA that can be translated and functions in Myogenesis. Mol Cell. 2017;66:22-37.

[2] Lasda E, Parker R. Circular RNAs: diversity of form and function. RNA. 2014;20:1829-42.

[3] Salzman J. Circular RNA expression: Its potential regulation and function. Trends Genet. 2016;32:309-16.

[4] Rybak-Wolf A, Stottmeister C, Glažar P, et al. Circular RNAs in the Mammalian Brain Are Highly Abundant, Conserved, and Dynamically Expressed. Mol Cell. 2015;58:870-85.

[5] Lukiw WJ. Circular RNA (circRNA) in Alzheimer's disease (AD). Front Genet. 2013;4:307.

[6] Hansen TB, Kjems J, Damgaard CK. Circular RNA and miR-7 in cancer. Cancer Res. 2013;73:5609–12.

[7] Li F, Zhang L, Li W, et al. Circular RNA ITCH has inhibitory effect on ESCC by suppressing the Wnt/β-catenin pathway. Oncotarget. 2015;6:6001–13.

[8] Li J, Yang J, Zhou P, et al. Circular RNAs in cancer: novel insights into origins, properties, functions and implications. Am J Cancer Res. 2015;5:472-80.

[9] Karoline K, Ebbesen Jørgen, Kjems. MicroRNA sponging by a new hearty circRNA.

Non-coding RNA Investigation. 2017;doi: 10.21037/ncri.2017.08.06.

[10] Yao Y, Charlesworth J, Nair V, et al. MicroRNA expression profiles in avian haemopoietic cells. Front Genet. 2013;4:153.

[11] Ambros V. The functions of animal microRNAs. Nature. 2004;431:350–355.

[12] Baek D, Villén J, Shin C, et al. The impact of microRNAs on protein output. Nature. 2008;455:64–71.

[13] Selbach M, Schwanhäusser B, Thierfelder N, et al. Widespread changes in protein synthesis induced by microRNAs. Nature. 2008;55:58–63.

[14] Bartel DP. MicroRNAs: target recognition and regulatory functions. Cell. 2009;136: 215–33.

[15] Liu AM, Poon RT, Luk JM. MicroRNA-375 targets Hippo-signaling effector YAP in liver cancer and inhibits tumor properties. Biochem. Biophys. Res. Commun. 2010;394: 623-27.

[16] Yan JW, Lin JS, He XX. The emerging role of miR-375 in cancer. Int. J. Cancer. 2014; 135:1011-18.

[17] Siow MY, Ng LP, Vincent-Chong VK, et al. Dysregulation of miR-31 and miR-375 expression is associated with clinical outcomes in oral carcinoma. Oral. Dis. 2014;20:345-51.

[18] Wang XZ, Hang YK, Liu JB, et al. Over-expression of microRNA-375 inhibits papillary thyroid carcinoma cell proliferation and induces cell apoptosis by targeting ERBB2. J Pharmacol Sci. 2016;130:78-84.

[19] Hansen TB, Jensen TI, Clausen BH, et al. Natural RNA circles function as efficient

microRNA sponges. Nature. 2013;495:384-88.

[20] Yu CY, Li TC, Wu YY, et al. The circular RNA circBIRC6 participates in the molecular circuitry controlling human pluripotency. Nat Commmun. 2017;8:1149.

[21] Bao Y, Hata Y, Ikeda M, et al. Mammalian Hippo pathway: from development to cancer and beyond. J. Biochem. 2011;149:361–79.

[22] Machado-Neto JA, Lazarini M, Favaro P, et al. ANKHD1, a novel component of the Hippo signaling pathway, promotes YAP1 activation and cell cycle progression in prostate cancer cells. Exp. Cell Res. 2014;324:137-45.

[23] Dong J, Feldmann G, Huang J, et al. Elucidation of a universal size-control mechanism in Drosophila and mammals. Cell. 2007;130:1120–33.

[24] Overholtzer M, Zhang J, Smolen GA, et al. Transforming properties of YAP, a candidate oncogene on the chromosome 11q22 amplicon. Proc Natl Acad Sci U S A. 2006;103:12405–10.

[25] Shao DD, Xue W, Krall EB, et al. KRAS and YAP1 converge to regulate EMT and tumor survival. Cell. 2014;158:171-84.

[26] De Craene B, Berx G. Regulatory networks defining EMT during cancer initiation and progression. Nat Rev Cancer. 2013;13:97–110.

[27] Yang J, Weinberg RA. Epithelial-Mesenchymal Transition: At the Crossroads of Development and Tumor Metastasis. Dev Cell. 2008;14:818-29.

[28] Gregory PA, Bert AG, Paterson EL, et al. The miR-200 family and miR-205 regulate epithelial to mesenchymal transition by targeting ZEB1 and SIP1. Nat Cell Biol. 2008;10:593-601.

[29] Wellner U, Schubert J, Burk UC, et al. The EMT-activator ZEB1 promotes tumorigenicity by repressing stemness-inhibiting microRNAs. Nat Cell Biol. 2009;11:1487-95.

[30] Duong TD, Erickson CA. MMP-2 plays an essential role in producing epithelial-mesenchymal transformations in the avian embryo. Dev Dyn. 2004;229:42-53.

[31] Díaz-López A, Moreno-Bueno G, Cano A. Role of microRNA in epithelial to mesenchymal transition and metastasis and clinical perspectives. Cancer Manag Res. 2014;6:205–16.

[32] Fadly A, Payne L. Leukosis/sarcoma group. In: Diseases of poultry, 11th ed. Saif YM, Barnes HJ, Glisson JR, et al, eds. Iowa State Press, Ames, IA. 2003;465-516.

[33] Stedman NL, Brwon TP. Body weight suppression in broilers naturally infected with avian leukosis virus subgroup J. Avian Dis. 1999;43:604-10.

[34] Du Y, Cui Z, Qin A. Subgroup J of avian leukosis viruses in China. China Poultry. 1999; 3:1-4.

[35] Payne LN, Nair V. The long view: 40 years of avian leukosis research. Avian Pathol. 2012;41:1–19.

[36] Reinišová M, Plachý J, Kučerová D, et al. Genetic diversity of NHE1, receptor for subgroup J avian leucosis virus, in domestic chicken and wild anseriform species. PLoS One. 2016;11:e0150589.

[37] Justice J4th, Malhotra S, Ruano M, et al. The MET gene is a common integration target in avian leukosis virus subgroup J-induced chicken hemangiomas. J Virol. 2015;89:4712-19.

[38] Li H, Shang H, Shu D, et al. gga-miR-375 plays a key role in tumorigenesis post subgroup J avian leukosis virus infection. PLoS One. 2014;9:e90878.

[39] Enright AJ, John B, Gaul U, et al. MicroRNA targets in Drosophila. Genome Biol. 2003;5:R1.

[40] Pasquinelli AE. MicroRNAs and their targets: recognition, regulation and an emerging reciprocal relationship. Nat Rev Genet. 2012;13:271-82.

[41] Zhang X, Yan Y, Lei X, et al. Circular RNA alterations are involved in resistance to avian leukosis virus subgroup-J-induced tumor formation in chickens. Oncotarget. 2017;8:34961-70.

[42] Jeck WR, Sorrentino JA, Wang K, et al. Circular RNAs are abundant, conserved, and associated with ALU repeats. RNA. 2013;19:141-57.

[43] Zheng Q, Bao C, Guo W, et al. Circular RNA profiling reveals an abundant circHIPK3 that regulates cell growth by sponging multiple miRNAs. Nat Commun. 2016;7:11215.

[44] Tang CM, Zhang M, Huang L, et al. CircRNA_000203 enhances the expression of fibrosis-associated genes by derepressing targets of miR-26b-5p, Col1a2 and CTGF, in cardiac fibroblasts. Sci Rep.2017;7:40342.

[45] He R, Liu P, Xie X, et al. circGFRA1 and GFRA1 act as ceRNAs in triple negative breast cancer by regulating miR-34a. J Exp Clin Cancer Res. 2017;36:145.

[46] Lee Y, Jeon K, Lee JT, et al. MicroRNA maturation: stepwise processing and subcellular localization. EMBO J. 2002;21:4663-70.

[47] Lytle JR, Yario TA, Steitz JA. Target mRNAs are repressed as efficiently by microRNA-binding sites in the 5' UTR as in the 3' UTR. Proc Natl Acad Sci U S A.

2007;104:9667-72.

[48] Jin Y, Chen Z, Liu X, et al. Evaluating the microRNA targeting sites by luciferase reporter gene assay. Methods Mol Biol. 2013;36:117-27.

[49] Nilsen TW. Mechanisms of microRNA-mediated gene regulation in animal cells. Trends Genet. 2007;23:243-49.

[50] Yang Z, Zhang X, Gang H, et al. Up-regulation of gastric cancer cell invasion by Twist is accompanied by N-cadherin and fibronectin expression. Biochem Biophys Res Commun. 2007;358:925-30.

[51] Fassina A, Cappellesso R, Guzzardo V, Dalla Via L, Piccolo S, Ventura L, Fassan M. Epithelial-mesenchymal transition in malignant mesothelioma. Mod Pathol. 2012;25:86-99.

[52] Friedl P, Gilmour D. Collective cell migration in morphogenesis, regeneration and cancer. Nat Rev Mol Cell Biol. 2009;10:445-57.

[53] Sarah Seton-Rogers. Oncogenes: All eyes on YAP1. Nature Reviews Cancer. 2014;14: 514-15.

[54] Shang X, Li G, Liu H, et al. Comprehensive circular RNA profiling reveals that hsa _circ_0005075, a new circular RNA biomarker, is involved in hepatocellular carcinoma development. Medicine (Baltimore). 2016;95:e3811.

[55] Wang X, Zhang Y, Huang L, et al. Decreased expression of hsa_circ_001988 in colorectal cancer and its clinical significances. Int J Clin Exp Pathol. 2015;8:16020-25.

[56] Sand M, Bechara FG, Gambichler T, et al. Circular RNA expression in cutaneous squamous cell carcinoma. J Dermatol Sci. 2016;83:210-18.

[57] Lin SP, Ye S, Long Y, et al. Circular RNA expression alterations are involved in OGD/R-induced neuron injury. Biochem Biophys Res Commun. 2016;471:52-56.

[58] Du WW, Yang W, Chen Y, et al. Foxo3 circular RNA promotes cardiac senescence by modulating multiple factors associated with stress and senescence responses. Eur Heart J. 2016;38:1402-12.

[59] Lu WY. Roles of the circular RNA circ-Foxo3 in breast cancer progression. Cell Cycle. 2017;16:589-90.

[60] Memczak S, Jens M, Elefsinioti A, et al. Circular RNAs are a large class of animal RNAs with regulatory potency. Nature. 2013;495:333–38.

[61] Fu L, Chen Q, Yao T, et al. Hsa_circ_0005986 inhibits carcinogenesis by acting as a miR-129-5p sponge and is used as a novel biomarker for hepatocellular carcinoma. Oncotarget. 2017;8:43878-88.

[62] Liu AM, Poon RT, Luk JM. MicroRNA-375 targets Hippo-signaling effector YAP in liver cancer and inhibits tumor properties. Biochem Biophys Res Commun. 2010;394:623-27.

[63] Li S, Yu Z, Chen SS, et al. The YAP1 oncogene contributes to bladder cancer cell proliferation and migration by regulating the H19 long noncoding RNA. Urol Oncol. 2015;33:427.e1-10.

[64] Lamar JM, Stern P, Liu H, et al. The Hippo pathway target, YAP, promotes metastasis through its TEAD-interaction domain. Proc Natl Acad Sci U S A. 2012;109:E2441–50.

[65] Zhang X, Yan Z, Li X, et al. GADD45β, an anti-tumor gene, inhibits avian leukosis virus subgroup J replication in chickens. Oncotarget. 2016;7: 68883-93.

[66] Gao Y, Yun B, Qin L, et al. Molecular epidemiology of avian leukosis virus subgroup J in layer flocks in China. J Clin Microbiol. 2012;50:953-60.

[67] Su H, Yang JR, Xu T, et al. MicroRNA-101, down-regulated in hepatocellular carcinoma, promotes apoptosis and suppresses tumorigenicity. Cancer Res. 2009;69:1135–42.

Figure legends

Figure 1. Bioinformatics analysis of differentially expressed circRNAs in tumor livers of ALV-J-susceptible chickens and normal livers of ALV-J-resistance chickens. (A) Normal liver (up) and tumor liver (down) in chickens infected with ALV-J. (B) Volcano plot of differentially expressed circRNAs in tumor livers and normal livers. (C) Scatter plot of differentially expressed circRNAs in tumor livers and normal livers. (D) Heap map for the 25 most significant differentially expressed circRNAs in tumor livers from circular RNA sequencing data. Sample [8], [14] and [9] represent ALV-J-susceptible chickens; [4], [3] and [26] represent ALV-J-resistant chickens. The numbers 0.0, 1.85 and 3.85 on the top represent the expression levels of the circRNAs. Each row represents a circRNA; each column represents one sample. Dendrograms produced by clustering analysis of the samples are shown on the top. (E) Predicted biomathematical circRNA-miRNA-gene network for the three-selected upregulated circRNAs, including circ-Vav3 (chr8:1033880-1047222-), in ALV-J-induced tumor livers. Yellow represents circRNAs, green represents miRNAs and pink represents miRNA target genes.

Figure 2. Circ-Vav3 sponges with gga-miR-375. (A) The Ensembl screen shot of the circ-Vav3 locus associated with the Vav3 gene. (B) Prediction and sequence analysis of gga-miRNA-375 response elements in circ-Vav3. The 2D structure shows the gga-miR-375 response element sequence and the target gga-miR-375 seed type (8-mer) and 3' pairing

sequence (nucleotides 13-16). The precise base positions are shown in the alignments in the upper left and right corners. (C and F) RIP assay shows that the miRNAs were successfully pulled-down using an AGO2 antibody. IgG was used as the negative control. (D, E, G and H) Fold enrichment of gga-miR-375 and circ-Vav3, respectively, quantified by RT-qPCR after RNA immunoprecipitation. GAPDH was the reference gene of circ-Vav3, U6 (figure D) and 5S (figure G) were used as the reference gene of gga-miR-375 (** represent $P < 0.01$). (I and J) Fold enrichment of gga-miR-375 quantified by RT-qPCR after circ-Vav3 pull-down. U6 (figure I) and 5S (figure J) were used as the reference gene of gga-miR-375 (** represent $P < 0.01$). (K) RNA *in situ* hybridization reveals the co-localization of circ-Vav3 and gga-miR-375 in the cytoplasm of DF-1 cells after the co-incubation of biotin-labeled circ-Vav3 and digoxin-labeled gga-miR-375 probes. Nuclei were stained with DAPI. Scale bar, 10 μm. The data represent the mean±s.e.m. of three independent experiments.

Figure 3. YAP1 mRNA as a direct target of gga-miR-375 and the effect of the transfection of gga-miR-375 on the EMT marker levels in DF-1 cells. (A) The complementary site for the seed region of gga-miR-375 is indicated after the alignment of the YAP1 3' UTR, gga-miR-375, and MUT 3' UTR. (B) Relative luciferase activity of YAP1 is dependent on gga-miR-375 (** represent $P < 0.01$). (C) The confirmation that gga-miR-375 was successfully overexpressed after transient transfection in DF-1 cells (** represent $P < 0.01$). (D) RT-qPCR reveals that the overexpression of gga-miR-375 downregulated the YAP1 mRNA expression at 24h (** represent $P < 0.01$). (E) Western blotting reveals that the overexpression of gga-miR-375 downregulated the YAP1 protein expression at 48h. The levels of YAP1 protein are shown as fold change next to the images after normalized with β-actin (**

represent $P < 0.01$). (F) Western blotting reveals that the overexpression of gga-miR-375 decreased the N-cadherin, Fibronectin, Vimentin, ZEB1 and MMP2 protein expression, but increased the E-cadherin protein expression compared with the mock-transfected cells at 48h. The levels of N-cadherin, Fibronectin, Vimentin, ZEB1, MMP2 and E-cadherin protein are shown as fold change next to the images after normalized with β-actin (** represent $P < 0.01$). (G) RT-qPCR revealed that the overexpression of gga-miR-375 decreased the level of N-cadherin (** represent $P < 0.01$), Fibronectin (** represent $P < 0.01$), Vimentin (** represent $P < 0.01$), ZEB1 (** represent $P < 0.01$), MMP2 (** represent $P < 0.01$), but increased that of E-cadherin (** represent $P < 0.01$) transcription compared to the mock-transfected cells at 24h. The data represent the mean±s.e.m. of three independent experiments.

Figure 4. Effects of YAP1 on cell migration and EMT in DF-1 cells. (A) The overexpression (OE) of YAP1 promoted DF-1 cell migration compared to the cells transfected with empty vector (EV) or the mock-transfected cells**.** (B) Relative cell migration ability of cells transfected with YAP1, EV- and mock-transfected cells (** represent $P < 0.01$). (C) The confirmation that YAP1 was successfully overexpressed in DF-1 cells (** represent $P < 0.01$). Immunoblotting revealed that the overexpression of YAP1 increased the N-cadherin, Fibronectin, Vimentin, ZEB1 and MMP2 protein expression, but decreased the E-cadherin protein expression compared with the mock-transfected cells at 48h. The levels of YAP1、N-cadherin, Fibronectin, Vimentin, ZEB1, MMP2 and E-cadherin protein are shown as fold change next to the images after normalized with β-actin (** represent $P < 0.01$). (D) RT-qPCR revealed that the overexpression of YAP1 increased the N-cadherin, Fibronectin, Vimentin,

ZEB1 and MMP2 transcription, but decreased the E-cadherin transcription compared with the mock-transfected cells (** represent $P < 0.01$) at 24h**.** The data represent the mean±s.e.m. of three independent experiments.

Figure 5. Co-transfection of circ-Vav3 and gga-miR-375 inducing EMT through enhancing YAP1 expression in DF-1 cell**s**. (A) PLCDH-circ-Vav3 was successfully overexpressed in DF-1 cells (** represent $P < 0.01$). (B) Changes in the expression of YAP1, EMT-associated marker proteins after the co-transfection of PLCDH-circ-Vav3 and gga-miR-375 at 48h. The levels of YAP1, EMT-associated marker proteins are shown as fold change next to the images after normalized with β-actin (** represent $P < 0.01$). (C) Changes in E-cadherin, N-cadherin and Fibronectin transcription after the co-transfection of PLCDH-circ-Vav3 and gga-miR-375 at 24h (** represent $P < 0.01$). (D) Changes in YAP1, Vimentin, ZEB1 and MMP2 transcription after the co-transfection of PLCDH-circ-Vav3 and gga-miR-375 at 24h (** represent $P < 0.01$). The data represent the mean±s.e.m. of three independent experiments.

Figure 6. Effects of the infection of ALV-J on the expression levels of circ-Vav3, gga-miR-375, YAP1 and EMT markers in DF-1 cells, and their expression levels in clinical liver samples**.** (A) Changes in circ-Vav3 transcription in DF-1 cells after infected with ALV-J at 0 and 12h (** represent $P < 0.01$). (B) Changes in gga-miR-375 transcription in DF-1 cells after infected with ALV-J at 0 and 12h (** represent $P < 0.01$). (C) Changes in the expression levels of YAP1 and EMT-associated marker proteins in DF-1 cells after infected with ALV-J at 48h. The levels of YAP1, EMT-associated marker proteins are shown as fold change next to the images after normalized with β-actin (** represent $P < 0.01$). (D) Changes in YAP1 transcription in DF-1 cells after infected with ALV-J at 24h (** represent $P < 0.01$). (E)

Changes in the transcription of EMT markers in DF-1 cells after infected with ALV-J at 24h (** represent $P < 0.01$). (F,G,H,I,J,K,L,M,N) The fold change of circ-Vav3, gga-miR-375, YAP1, Fibronectin, N-cadherin, E-cadherin, Vimentin, ZEB1 and MMP2, respectively in clinical ALV-J-induced tumor livers and normal livers (** represent $P < 0.01$). The data represent the mean±s.e.m. of three independent experiments.

Figure 7. Mechanism of tumorigenesis in chickens after infected with ALV-J. In host cells infected with the virus, the up-regulated circ-Vav3 increased the adsorption of gga-miR-375 through the miRNA sponge function, and further relieved the inhabitation of the gga-miR-375 target gene-YAP1. The increased accumulation of YAP1 can promote tumorigenesis through inducing EMT by affecting the mesenchymal markers-N-cadherin, Fibronectin, Vimentin, ZEB1, MMP2 and the epithelial marker-E-cadherin.

Table 1. The 25 upregulated and differentially expressed circRNAs in ALV-J-induced tumor livers.

Name	Fold change	*P* value	Catalog	Best related linear transcript (Gene symbol)	Gene names
chr5:22838365-22845389+	2.251548	0.002486	exonic	ENSGALT00000038392	AMBRA1
chr23:2553492-2553764+	5.003931	0.004175	intronic	NM_204492	PTPRU
chr3:107001245-107001722-	3.099086	0.026882	exonic	NM_205371	CTSB
chr8:6335683-6342031-	4.177297	0.010604	exonic	NM_001006532	RALGPS2
chr2:129790014-129796162-	4.952734	0.014766	exonic	ENSGALT00000025906	LRP12
chr15:510690-523720+	5.143408	0.025829	sense overlapping	NM_204150	MAPK1
chr4:59505289-59510641-	6.342368	0.029650	sense overlapping	ENSGALT00000045990	EIF4E
chr28:2923736-2928947+	5.540568	0.048443	exonic	NM_001045833	STK11
chr2:102577691-102580382+	3.049092	0.038400	exonic	ENSGALT00000024186	CABLES1
chr4:4236256-4238806-	4.245790	0.021676	exonic	ENSGALT00000010111	MAP7D3
chr1:193288082-193294652-	3.566240	0.032924	exonic	NM_001030839	UVRAG
chr3:3137166-3138170+	4.493181	0.028216	exonic	NM_204988	MERTK
chr3:15974512-15976254-	4.082326	0.010605	exonic	ENSGALT00000021600	SOS1
chr3:98482045-98486420-	3.049092	0.010568	exonic	ENSGALT00000026557	NBAS
chr9:15310869-15311235+	5.327255	0.004786	exonic	NM_001079494	AP2M1
chr5:51521674-51524828-	11.26283	0.008252	exonic	NM_205055	AKT1
chr19:7394013-7394212-	3.240144	0.044276	antisense	NM_001030721	RPS6KB1
chr18:11019600-11024292-	2.830527	0.026031	exonic	NM_204411	GRB2
chr17:622167-627777-	2.246590	0.017298	exonic	ENSGALT00000014614	RABL6
chr13:13265658-13271996+	2.830527	0.026031	exonic	NM_205095	MAPK9
chr1:14219949-14223612+	2.830527	0.026031	exonic	NM_001199538	PIK3CG
chr3:101911728-101911843-	2.246590	0.017298	exonic	NM_001044633	APOB
chr22:214764-230476-	2.246590	0.028824	exonic	ENSGALT00000000136	ANTXR1
chr8:1033880-1047222-	2.246590	0.021845	exonic	NM_206863	VAV3
chr2:145294919-145302275-	3.240144	0.000673	exonic	NM_205435	PTK2

Table 2. The binding scores of the top five predicted miRNAs for the 25 upregulated and differentially expressed circRNAs in ALV-J-induced tumor livers.

CircRNA ID	miRNA (structure score)	miRNA (structure score)	miRNA (structure score)	miRNA (structure score)	miRNA (structure score)
chr15:510690-523720+	gga-miR-6640-5p (1296)	gga-miR-106-3p (1184)	gga-miR-1551-5p (1182)	gga-miR-1688 (1179)	gga-miR-1793 (1043)
chr5:51521674-51524828-	gga-miR-6675-3p (159)	gga-miR-7463-5p (155)	gga-miR-1643-5p (155)	gga-miR-1698 (154)	gga-miR-456-5p (151)
chr28:2923736-2928947+	gga-miR-20a-3p (432)	gga-miR-6665-5p (309)	gga-miR-1730-3p (306)	gga-miR-6646-3p (302)	gga-miR-6623-3p (301)
chr4:4236256-4238806-	gga-miR-1651-3p (462)	gga-miR-7450-5p (160)	gga-miR-1600 (157)	gga-miR-1748 (153)	gga-miR-1641 (152)
chr18:11019600-11024292-	gga-miR-6573-5p (163)	gga-miR-6619-5p (163)	gga-miR-1573 (157)	gga-miR-187-3p (157)	gga-miR-1785 (154)
chr8:1033880-1047222-	gga-miR-375 (161)	gga-miR-1712-5p (154)	gga-miR-7459-5p (153)	gga-miR-1416-3p (152)	gga-miR-6579-3p (151)
chr3:3137166-3138170+	gga-miR-7449-3p (159)	gga-miR-6663-5p (156)	gga-miR-1586 (152)	gga-miR-1803 (150)	gga-miR-1464 (148)
chr1:14219949-14223612+	gga-miR-1627-5p (305)	gga-miR-1799 (296)	gga-miR-6545-5p (293)	gga-miR-1753 (286)	gga-miR-6552-3p (168)
chr2:129790014-129796162-	gga-miR-1806 (158)	gga-miR-6678-3p (156)	gga-miR-1565 (155)	gga-miR-211 (155)	gga-miR-204 (155)
chr19:7394013-7394212-	gga-miR-2128 (169)	gga-miR-1662 (161)	gga-miR-1811 (157)	gga-miR-184-5p (157)	gga-miR-1598 (154)
chr4:59505289-59510641-	gga-miR-757 (745)	gga-miR-29b-1-5p (618)	gga-miR-1705 (593)	gga-miR-1804 (581)	gga-miR-1762 (574)
chr23:2553492-2553764+	gga-miR-6698-3p (169)	gga-miR-20b-5p (163)	gga-miR-17-5p (163)	gga-miR-106-5p (163)	gga-miR-6587-5p (162)
chr9:15310869-15311235+	gga-miR-6578-3p (293)	gga-miR-6700-3p (165)	gga-miR-6552-5p (162)	gga-miR-7473-5p (159)	gga-miR-6582-3p (158)
chr17:622167-627777-	gga-miR-140-5p (157)	gga-miR-1744-3p (154)	gga-miR-1654 (153)	gga-miR-302b-5p (152)	gga-miR-1815 (151)
chr3:101911728-101911843-	gga-miR-6551-3p (151)	gga-miR-7450-3p (150)	gga-miR-30e-5p (149)	gga-miR-30c-5p (146)	gga-miR-30b-5p (146)
chr22:214764-230476-	gga-miR-148a-5p (429)	gga-miR-6584-5p (320)	gga-miR-1611 (298)	gga-miR-205b (293)	gga-miR-1626-3p (292)
chr5:22838365-22845389+	gga-miR-7448-5p (170)	gga-miR-6679-5p (158)	gga-miR-4732-5p (158)	gga-miR-1762 (158)	gga-miR-200b-3p (155)
chr3:98482045-98486420-	gga-miR-7450-5p (282)	gga-miR-6673-3p (164)	gga-miR-6655-5p (163)	gga-miR-6577-5p (157)	gga-miR-7464-5p (155)
chr2:102577691-102580382+	gga-miR-1754-5p (157)	gga-miR-6673-3p (149)	gga-miR-148a-5p (147)	gga-miR-7470-5p (145)	gga-miR-1662 (144)
chr3:107001245-107001722-	gga-miR-383-3p	gga-miR-6607-5p	gga-miR-1756b	gga-miR-1665	gga-miR-1608

	(296)	(158)	(157)	(155)	(155)
chr13:13265658-13271996+	gga-miR-190a-5p	gga-miR-365-1-5p	gga-miR-7483-5p	gga-miR-217-3p	gga-miR-146b-3p
	(290)	(281)	(168)	(164)	(160)
chr2:145294919-145302275-	gga-miR-29b-1-5p	gga-miR-29b-2-5p	gga-miR-1656	gga-miR-1716	gga-miR-9-5p
	(454)	(449)	(298)	(292)	(285)
chr1:193288082-193294652-	gga-miR-1564-3p	gga-miR-7479-3p	gga-miR-1416-3p	gga-miR-1731-5p	gga-miR-9-5p
	(320)	(301)	(295)	(292)	(289)
chr3:15974512-15976254-	gga-miR-19b-5p	gga-miR-19a-5p	gga-miR-23b-5p	gga-miR-1710	gga-miR-6577-5p
	(447)	(431)	(317)	(306)	(301)
chr8:6335683-6342031-	gga-miR-7481-3p	gga-miR-1685-5p	gga-miR-7462-5p	gga-miR-1645	gga-miR-7483-3p
	(290)	(166)	(160)	(157)	(156)

Table 3. Primers are used for RT-qPCR in this study.

Gene names	Primers
circ-Vav3	F: AGACACGTGGACCCAGGTCA
	R: CAGACTTTGCAGGACGTCACAC
gga-miR-375	TgTTcgTTcggcTcgcgTTa
YAP1	F: GAACTCAGCATCAGCCATGA
	R: CTACGGAGAGCCAATTCCTG
Fibronectin	F: TGGAAAGCGTCGATGACACA
	R: GAACACCTGGCATCAGGTCA
N-cadherin	F: TGGATGAAGCGCCGTGATAA
	R: AGGTTTGATGGCGTCTGGTT
E-cadherin	F: GAAGACAGCCAAGGGCCTG
	R: GGGCCGTGTAGGATGTAACC
5s	TTAGCTTCCGAGATCAGACG
β-actin	F: CTGGCACCTAGCACAATGAA
	R: CTGCTTGCTGATCCACATCT
GAPDH	F: TGCCATCACAGCCACACAGAAG
	R: ACTTTCCCCACAGCCTTAGCAG

Table 4. Primers are used for RIP and RNA pull down in this study.

Gene names	Primers
circ-Vav3	F: GCGCACAAAGAATGTTTAGGA
	R: GGACGTCACACGACTGAAAG
gga-miR-375	F: GGGTTTGTTCGTTCGGCTC
	R: CAGTGCGTGTCGTGGAGT
U6	F: CTCGCTTCGGCAGCACA
	R: CGCTTCACGAATTTGCGTGTCAT
5S	TTAGCTTCCGAGATCAGACG
GAPDH	F: CCTCTCTGGCAAAGTCCAAG
	R: CATCTGCCCATTTGATGTTG

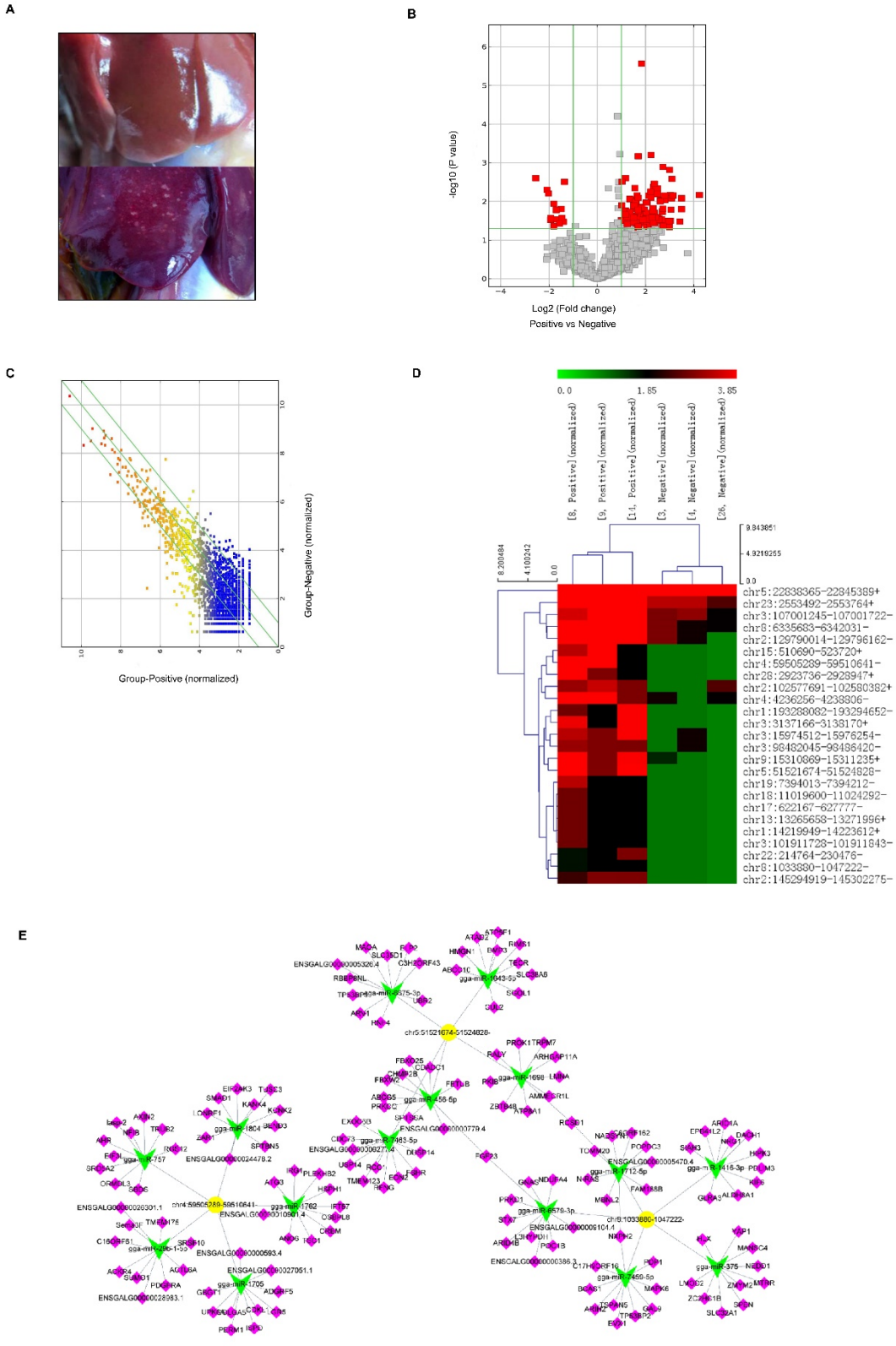
A
B
-log10 (P value)
Log2 (Fold change)
Positive vs Negative
C
Group-Negative (normalized)
Group-Positive (normalized)
D
[8, Positive] (normalized)
[9, Positive] (normalized)
[11, Positive] (normalized)
[3, Negative] (normalized)
[4, Negative] (normalized)
[26, Negative] (normalized)
chr5:22838365-22845389+
chr23:2553492-2553764+
chr3:107001245-107001722-
chr8:6335683-6342031-
chr2:129790014-129796162-
chr15:510690-523720+
chr4:59505289-59510641-
chr28:2923736-2928947+
chr2:102577691-102580382+
chr4:4236256-4238806-
chr1:193288082-193294652-
chr3:3137166-3138170+
chr3:15974512-15976254-
chr3:98482045-98486420-
chr9:15310869-15311235+
chr5:51521674-51524828-
chr19:7394013-7394212-
chr18:11019600-11024292-
chr17:622167-627777-
chr13:13265658-13271996+
chr1:14219949-14223612+
chr3:101911728-101911843-
chr22:214764-230476-
chr8:1033680-1047222-
chr2:145294919-145302275-
E

Figure 1

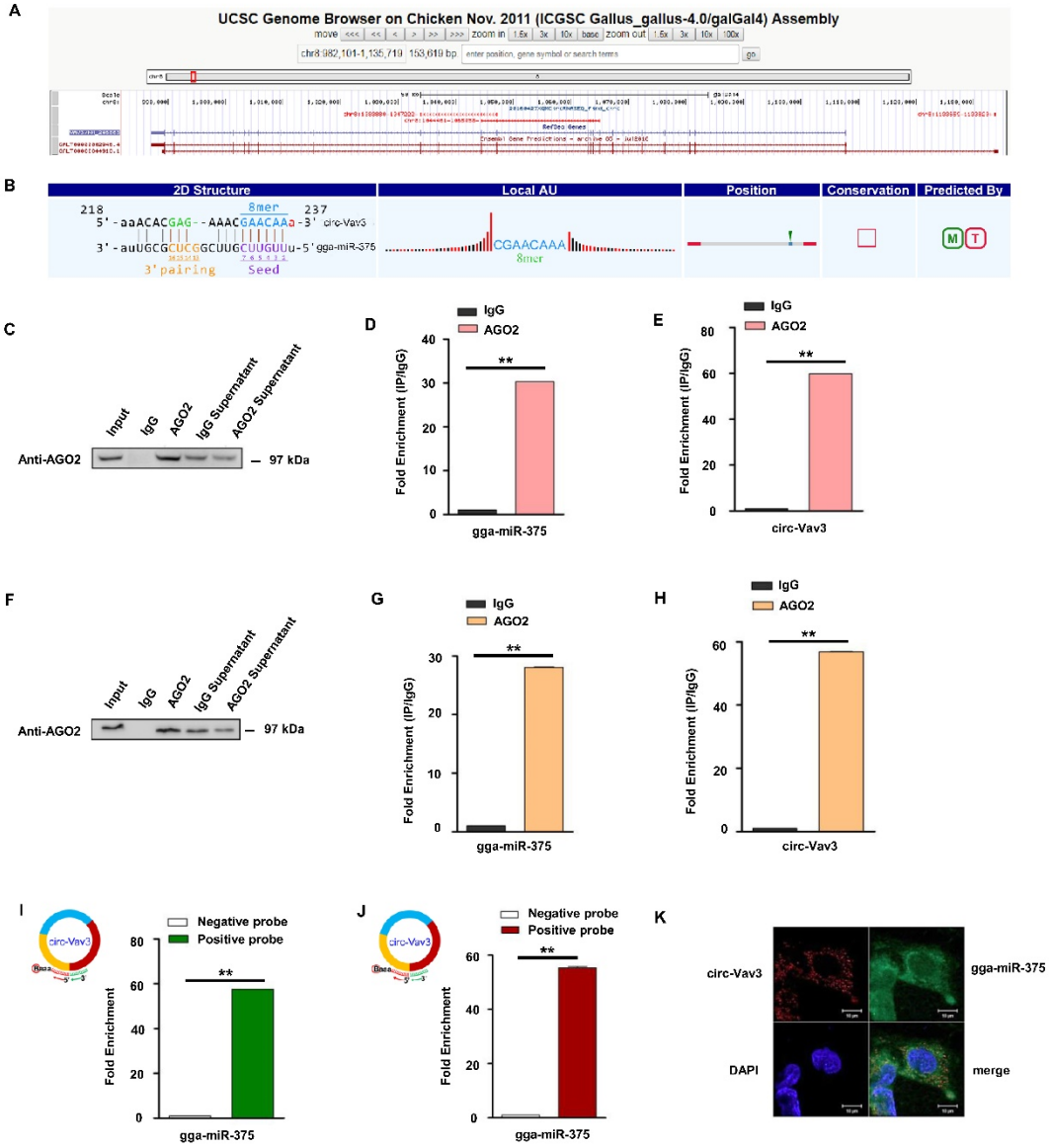

Figure 2

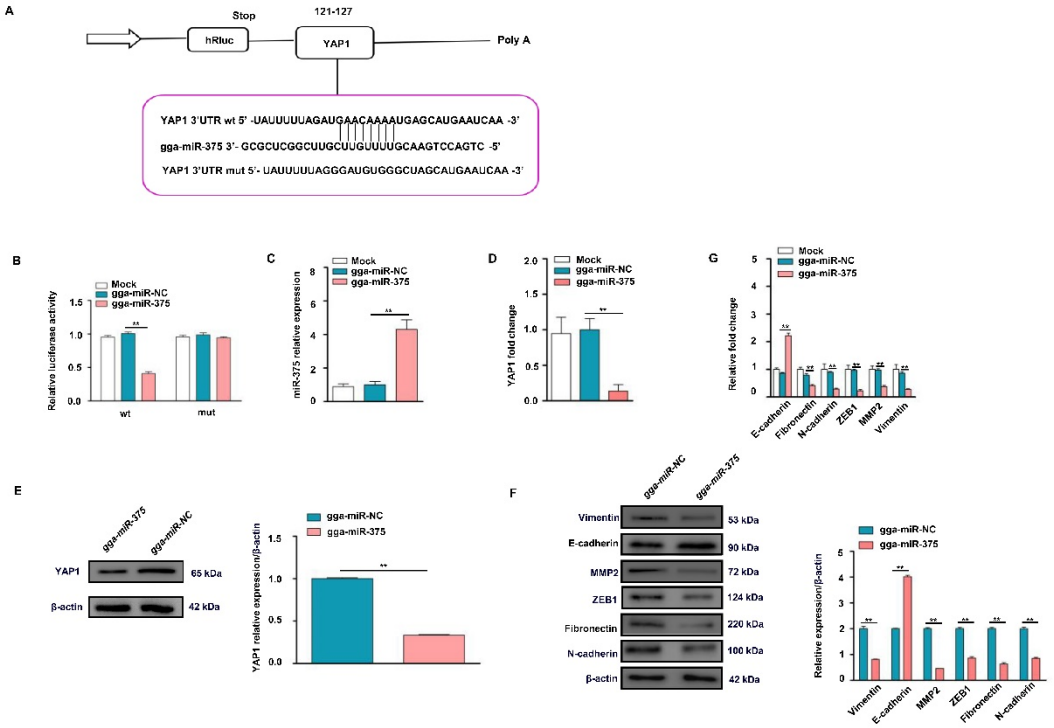

Figure 3

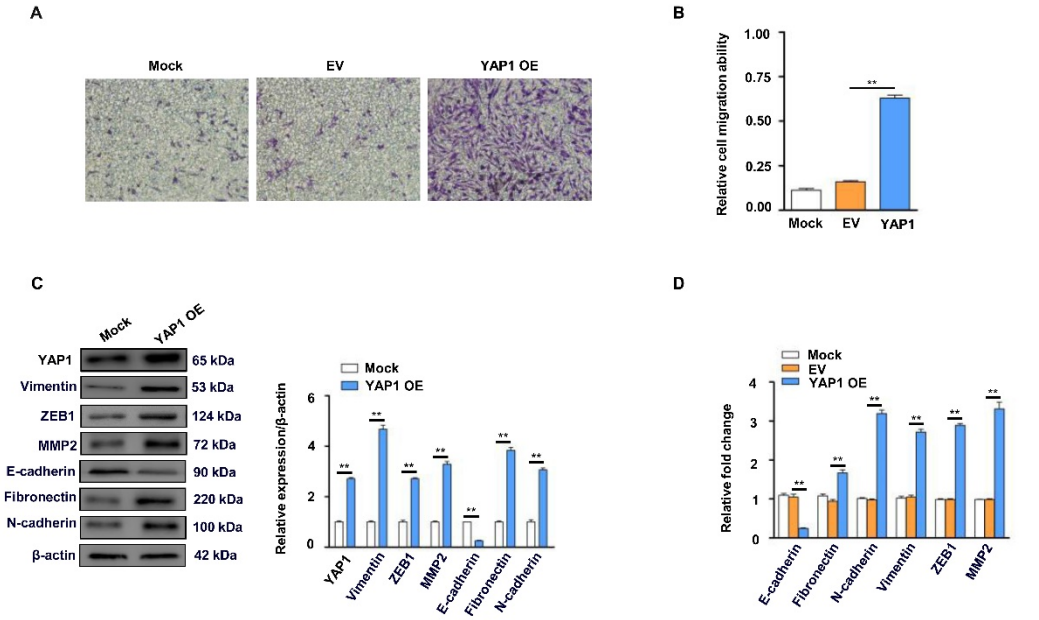

Figure 4

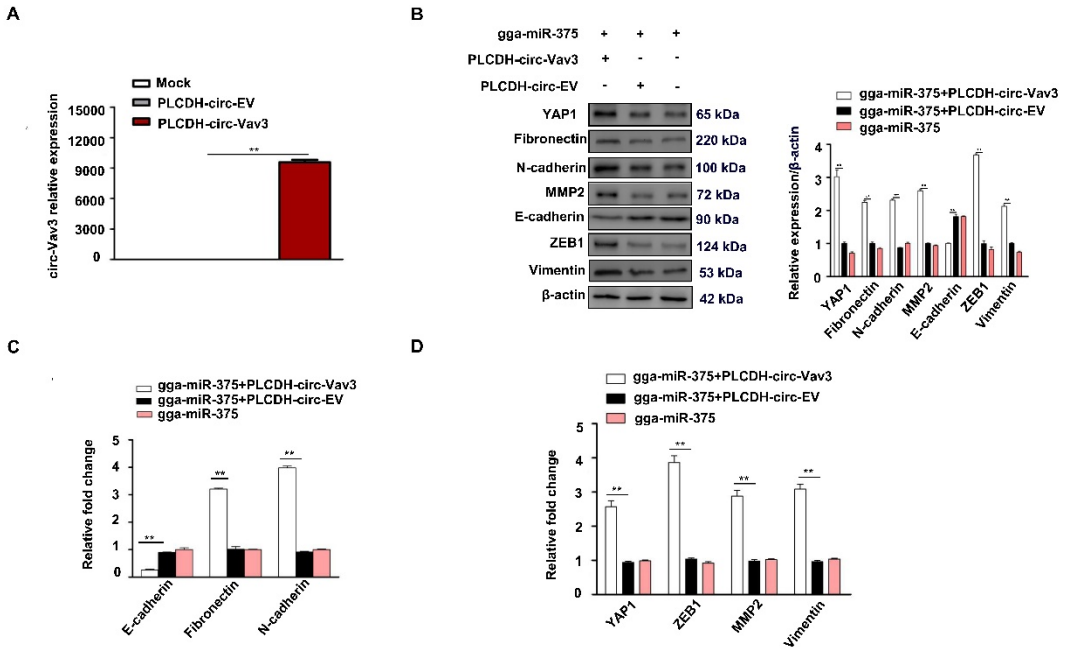

Figure 5

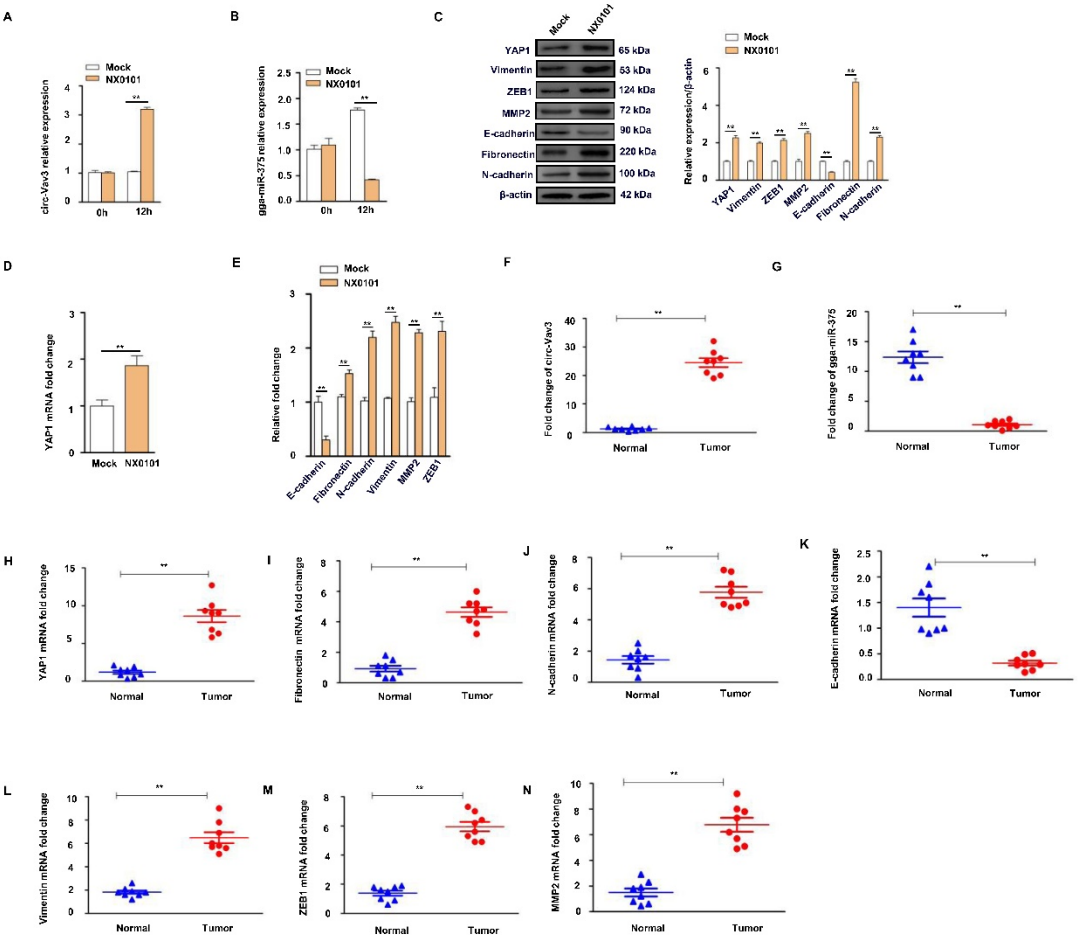

Figure 6

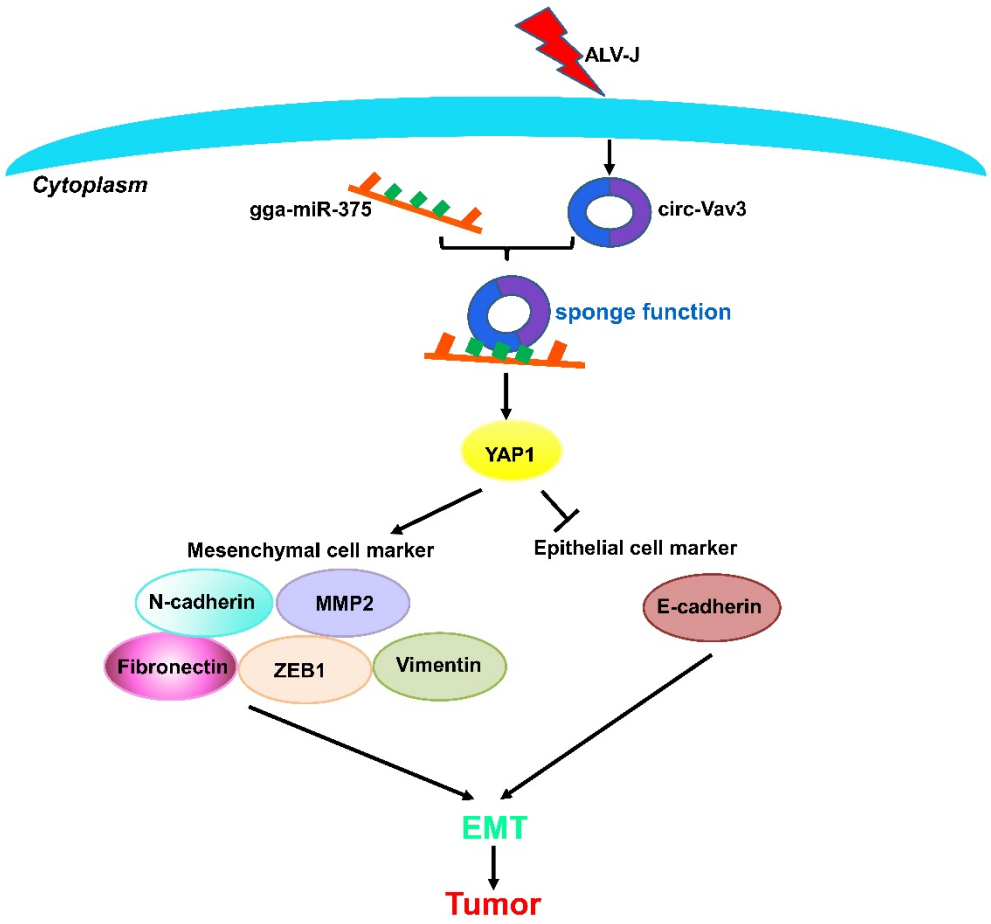

Figure 7